# Combination of permanent hydrosilylation and reversible Diels-Alder reactions for self-healing PDMS materials with enhanced ageing properties

Dijwar Yilmaz[a,b,c], David Lansade[a,b,c*], Simon Lewandowski[a], Sophie Perraud[b], Audrey Llevot[c], Stéphane Carlotti[c*].

[a] ONERA / DPHY, Université de Toulouse F31055 Toulouse, France

[b] CNES – French Aerospace Agency, 18 avenue Edouard Belin F-31401 Toulouse Cedex 9, France

[c] Univ. Bordeaux, CNRS, Bordeaux INP, LCPO, UMR 5629, F-33600, Pessac, France

*Corresponding author. E-mail addresses stephane.carlotti@enscbp.fr, david.lansade@onera.fr

**Keywords:** Remendable polymers, PDMS, Double network, Proton irradiation, Karstedt's catalyst, Furan-maleimide chemistry

## ABSTRACT

Poly(dimethylsiloxane)s (PDMS) are widely used in space applications thanks to their transparency, thermal and UV resistance, *inter alia*. The prolonged exposure of these materials to the geostationary environment leads to the apparition of cracks and changes in their optical properties, this being detrimental to their function. In order to enhance their lifespan, self-healing PDMS based on a dual network featuring both permanent and reversible units thanks to hydrosilylation and Diels-Alder reactions were designed. The tunable chemical composition of the networks was characterized by proton Nuclear Magnetic Resonance spectroscopy ($^1$H NMR) and Fourier Transformed Infra-Red-Attenuated Total Reflection (FTIR-ATR)

measurements. The thermal and mechanical behaviors of pristine and healed materials were mainly studied by Differential Scanning Calorimetry (DSC), Dynamic Mechanical Analysis (DMA) and tensiometry. Ageing under proton irradiations was also performed, simulating part of the radiations encountered in geostationary environment. Ultraviolet-Visible-Near Infrared (UV-Vis-NIR) analyses were carried out to compare the materials optical properties both before and after irradiations. Finally, chemical degradation mechanisms were studied by FTIR-ATR analyses and discussed.

## 1. Introduction

Due to their inorganic backbone, poly(dimethylsiloxane)s (PDMS) are known to differ from carbon-based polymers. They possess unique properties such as a high degradation temperature (~ 400 °C), a very low $T_g$ (~ -120 °C), high elasticity as well as transparency in a wide spectroscopic range. Thanks to these properties, PDMS are widely used as adhesives[1,2,3], solar panel coatings[4,5,6], biomedical applications[7,8], microfluidics devices[9,10,11]…

As a result, understanding their degradation and extending their lifespan is of primary importance in many industries. In space applications, exposure to proton or electron irradiations leads to the formation of cracks on the surface of this type of materials, reducing their mechanical and optical performances[12,13]. As the material cannot be easily accessed for replacement, a strategy leading to a reduction of these degradations may improve the lifespan of the device. One general approach to solve this issue is the stabilization of the material by embedding inorganic nanoparticles in its surface, which acts as a protection of the polymeric matrix[4,5,14]. Another innovative approach to enhance the lifetime of PDMS for general purposes consists in implementing the concept of self-healing. Different types of self-healing systems were explored in the literature, namely extrinsic and intrinsic. On the one hand, extrinsic self-

healing requires an external agent, usually encapsulated in a polymeric matrix, to repair the damaged region. In 2006, Braun *et al.* designed a self-healing PDMS in which was embedded a di-*n*-butyltin di-laurate (DBTL) catalyst that could be released on crack appearance[15]. This catalyst would induce the polycondensation of hydroxy end-functionalized PDMS and PDMS already present in the matrix, so as to repair the deteriorated region. However, by design, this system is composed of a fixed amount of self-healing agents leading to a limited repairing of the matrix.

On the other hand, intrinsic self-healing PDMS involves chemical interactions ranging from non-covalent interactions such as hydrogen bonding[16,17] , $\pi$-$\pi$ stacking[18], metal-ligand[19,20,21,22], guest-host chemistry[23] or ionic[24] to dynamic covalent bonds often being disulfide bridges[25,26,27], imines[28,29,30] or urea[31,32] functions, as well as Diels-Alder adducts[33,34].

The Diels-Alder (DA) reaction based on a [4+2] cycloaddition is well known for self-healing applications due to its thermal responsiveness[35,36]. By adjusting the temperature, the cycloadduct can be formed by DA reaction (60-80 °C) or broken when heated to the appropriate temperature (120-140 °C) by retro Diels-Alder (rDA). This reversibility is expected to heal cracks and boost materials life. The pioneering work in DA reactions for self-healable polymers has been carried out by Wudl *et al.* in 2002, who showed the potential of this system by constructing and deconstructing a molecular network with small molecules containing 3 maleimide and 4 furan groups[37] . Since then, DA chemistry was applied to a large panel of different polymer systems, including diene elastomers[38–44], polyurethanes[31,45–50] or silicone elastomers[34,51–53].

Recently, Zhao *et al.* reported a facile route to prepare self-healing PDMS by crosslinking furan-terminated PDMS with PDMS bearing pendant maleimide functions[54]. Hydrogen bonds formed between adjacent maleimide moieties were also shown to increase mechanical

properties of the system[54,55]. However, such DA systems are not stable upon temperature. Above rDA temperature, a loss of integrity of the polymer network is observed, causing the material to flow. This challenge can be tackled by complementing the DA cross-linking points with static covalent crosslinks[33], thus forming double polymer networks.

The application of these double networks for DA systems has been developed recently[56,57]. The incorporation of acrylate monomers into DA network was proposed by Bowman and collaborators to prepare a permanent/reversible double network, the permanent part being obtained by UV irradiation[58]. Interestingly, Huang *et al.* added hyperbranched polysiloxanes, obtained through hydrolysis condensation reactions, to a DA network in order to improve the mechanical properties of their materials[33].

Herein are reported the synthesis, physico-chemical characterization and ageing under proton irradiations of a doubly cross-linked PDMS, associating both the advantages of the Diels-Alder reversibility and the mechanical properties of a permanently cross-linked matrix obtained by hydrosilylation.

## 2. Experimental section

### 2.1 Materials

Aminopropylmethylsiloxane-dimethylsiloxane copolymer (AMS-163) containing 6-7 % of aminopropylmethylsiloxane ($\overline{M_w}$ ~ 50000 g.mol$^{-1}$), aminopropyl-terminated poly(dimethylsiloxane) DMS-A12, ($\overline{M_w}$ ~ 900-1000 g.mol$^{-1}$), hydride-terminated poly(dimethylsiloxane) DMS-H11 ($\overline{M_w}$ ~ 1000-1100 g.mol$^{-1}$) were purchased from Gelest (USA). 2-furoyl chloride (> 98 %) and allyl bromide (99 %) were both purchased from Alfa Aesar. 1,8-Diazabicyclo[5.4.0]undec-7-ene (DBU, > 98 %) was purchased from TCI.

Platinium-divinyltetramethyldisiloxane complex in xylene (2,1-2,4 % Pt) was purchased from ABCR. Maleic anhydride, magnesium sulfate, sodium chloride, and glacial acetic acid were all purchased from Sigma-Aldrich. MAPSIL®QS1123 was prepared by mixing a base containing vinyl-terminated PDMS and Pt catalyst (Karstedt catalyst) with hydride-based siloxane as the hardener in 10:1 weight ratio, both provided by MAP. All reagents were used as received, without further purification.

**2.2 Synthesis of PDMS base**

AMS-163 (10 g, 8.6 mmol of $NH_2$, 1 eq), DBU (1.44 g, 9.46 mmol, 1.1 eq) were added to dry THF (70 mL) under argon atmosphere. After homogenization, allyl bromide (0.104 g, 0.86 mmol, 0.1 eq) was added under inert atmosphere. The mixture was heated at 65 °C for 15 hours under magnetic stirring. The crude product was filtrated to remove DBU salts and THF was removed using rotatory evaporator. Then, the polymer was dissolved in $CH_2Cl_2$, washed 3 times with sodium chloride saturated aqueous solution (3 x 100 mL), dried with $MgSO_4$, and filtered again. The pre-base was obtained after being dried overnight. The steps above described will be called “Purification Steps” in the rest of the article. NMR showed in this case that 80 % of initially introduced allyl were incorporated into the polymer.

The same protocol was then followed to introduce furan moieties. The pre-base synthesized previously (8.47 g, 7.28 mmol, 1 eq), DBU (1.22 g, 8.01 mmol, 1.1 eq) and dry THF (70 mL) were introduced in a 100 mL Schlenk flask. 2-furoyl chloride (0.856 g, 6.55 mmol, 0.9 eq,) was added dropwise to the mixture previously placed in an ice bath. Very quickly, the content of the flask became white and turbid. It was then stirred for 24 hours at room temperature. Purification steps were applied to the white solution. Different bases with various allyl and furan percentages were synthesized. Their content in allyl moieties ranged from 0 to 100 % while their furan’s one ranged from 8 to 100 %, as compared to the amount of primary amines

originally present in the AMS-163 commercial polymer. The incorporation of allyl and furan moieties were controlled by $^{1}$H NMR in E.S.I., Figure S1.

$^{1}$H NMR spectroscopy (400 MHz; $CDCl_3$): δ (ppm): 8.5-8.25 (s, -N**H**-C=O, 11H), 7.41 (s, =C**H**-O, 86H), 7.09 (s, -C**H**=C-O, 86H), 6.48-6.39 (m, =C**H**-CH=, 162H), 5.85 (s, $CH_2$=C**H**-, 7H), 5.21-5.17 (d, C**H**$_2$=CH-, 8H), 4.16-4.0 (m, NH-C**H$_2$**-CH=$CH_2$, 15H), 3.51-3.31(m, Si-$CH_2$-$CH_2$-C**H$_2$**-NH, 200H), 1.80-1.53 (m, NH-$CH_2$-C**H$_2$**-$CH_2$-Si-, 234H), 0.64-0.39 (m, -Si-C**H$_2$**-$CH_2$-$CH_2$-, 200H), 0.28-0.00 (m, C**H$_3$**-Si-, 10230H)

### 2.3 Synthesis of PDMS "reversible" hardener

DMS-A12 (20 g, 4.44x10$^{-2}$ mol of primary amine, 1 eq) was dissolved in glacial acetic acid (150 mL) in a 250 mL round bottom flask. Maleic anhydride (21.79 g, 2.22x10$^{-1}$ mol, 5 eq) was added to the flask and the mixture was heated under reflux at 140 °C for 6 hours. To remove acetic acid, Purification Steps were applied. Finally, the PDMS "reversible" hardener was obtained after being dried overnight under vacuum.

$^{1}$H NMR spectroscopy (400 MHz; $CDCl_3$): δ (ppm): 6.67 (s, -C**H**=C**H**-C=O, 1H), 3.5 (t, -N-C**H$_2$**-$CH_2$-$CH_2$-Si-, 1H), 1.6 (m, N-$CH_2$-C**H$_2$**-$CH_2$-Si-, 1H), 0.5 (m, N-$CH_2$-$CH_2$-C**H$_2$**-Si-, 1H), 0.17-0.00 (m, C**H$_3$**-Si-, 34H).

### 2.4 Elaboration of "self-healing" resins

The degrees of functionalization of PDMS base and PDMS "reversible" hardener were controlled by $^{1}$H NMR spectroscopy. To make resins, stoichiometric amounts of base and hardener were mixed in a vial: 2 g of base, 1.72 g of PDMS "reversible" hardener, and 0.172 g of PDMS permanent hardener (DMS-H11) were mixed together. Karstedt's catalyst was added in excess and the mixture was stirred manually. To avoid the presence of air and remove any trace of solvent, the vial was left under vacuum before being poured in a mold in order to make

thick films. The mold was heated at 70 °C for 48 hours in order to crosslink the system, allowing hydrosilylation and Diels-Alder reactions to occur. The films obtained were orange and transparent.

In the rest of this article, the notation PDMS-$DA_x$-$Allyl_y$ (x and y being the proportion of furane and allyl moieties along the backbone of the base used to make the resin, as determined by $^1H$ NMR spectroscopy) will be used to name the obtained resins.

**2.5 Characterization of materials**

Liquid-state $^1H$ NMR spectra were recorded at 298 K on a Bruker Avance 400 spectrometer operating at 400 MHz, in $CDCl_3$. Differential scanning calorimetry (DSC) measurements of PDMS samples (~ 10 mg) were performed using a DSC Q100 $LN_2$ apparatus from TA Instruments with heating and cooling ramps of 10 °C.min$^{-1}$. The samples were first heated from 25 to 100 °C and held at 100 °C for 10 min in order to eliminate any residual solvent, then cooled to -130 °C, and finally heated to 200 °C. The analyses were carried out under helium atmosphere in aluminum pans. Fourier transform infrared (FTIR) spectra were recorded on a Bruker VERTEX 70 instrument (4 cm$^{-1}$ resolution, 32 scans, DLaTGS MIR) equipped with a Pike GladiATR plate (diamond crystal) for attenuated total reflectance (ATR) at room temperature. UV-Vis-NIR analyses were performed on a PerkinElmer lambda 1050 in the 250 to 2500 nm range on a transmission mode (1 nm resolution, 250 nm.min$^{-1}$ scanning speed). A TA Instrument DMA 850 (dynamic mechanical analysis) was used to study the thermo-mechanical properties of 15 mm diameter, 3 mm thick PDMS disks from -130 °C to 200 °C at a heating rate of 3 °C.min$^{-1}$. The measurements were performed in compression tests at a frequency of 1 Hz, a strain sweep of 0.2 % (linear domain) and an initial static force of 1 N. Tensile strength and percentage of elongation were measured by a MTS Qtest 25 Elite controller (France). PDMS samples were cut in bars (5 mm width x 20 mm long) and remolded

using a heat press (at 10 bars) for 1 hour and left at 70 °C for 48 hours in an oven before measurements. The initial grip separation was set at 15 mm and the crosshead speed at 1.0 $mm.min^{-1}$. The tests were performed on 7 to 8 replicates. SEMIRAMIS facility present at ONERA was used for ageing under proton irradiation. It consists in a 2.5 MeV Van de Graaf proton accelerator coupled with a high vacuum enclosure, containing the sample holder with polymer films (20 mm x 20 mm x 1 mm). The chamber was kept at 40 °C with a pressure under $10^{-5}$ mbar. The proton flux was $9.42x10^{10}$ $p^+.cm^{-2}.s^{-1}$ (15 $nA.cm^{-2}$) with an energy of 240 keV. The total fluence was $3x10^{15}$ $p^+.cm^{-2}$ for a total surface dose of $2x10^8$ Gy. The swelling properties of PDMS-$DA_x$-$Allyl_y$ were also tested. Three pieces of resins of about 100 mg each were weighted ($m_0$), and immersed in THF for 24 hours. The swollen samples were lightly dried with paper and weighted again ($m_S$). The swelling ratio was calculated according to the following equation:

$$\text{Swelling ratio} = \frac{(m_S - m_0)}{m_0} \quad (1)$$

Finally, the samples were left to dry in an oven at 70 °C for 24 hours and weighted ($m_D$). The insoluble fraction of the network was calculated from the following equation:

$$\text{Insoluble fraction} = \frac{m_D}{m_0} \quad (2)$$

**3. Results and discussion**

With the objective to prepare poly(dimethylsiloxane) resins with self-healing properties while keeping their mechanical properties, a PDMS featuring $NH_2$ pendant groups (~7 %) was chemically modified by the introduction of various percentages of allyl and furan moieties (Scheme 1). A two-step procedure was implemented involving a substitution reaction with allyl

bromide followed by an amidation of the remaining free $NH_2$ with 2-furoyl chloride. These two steps were organo-catalyzed by DBU.

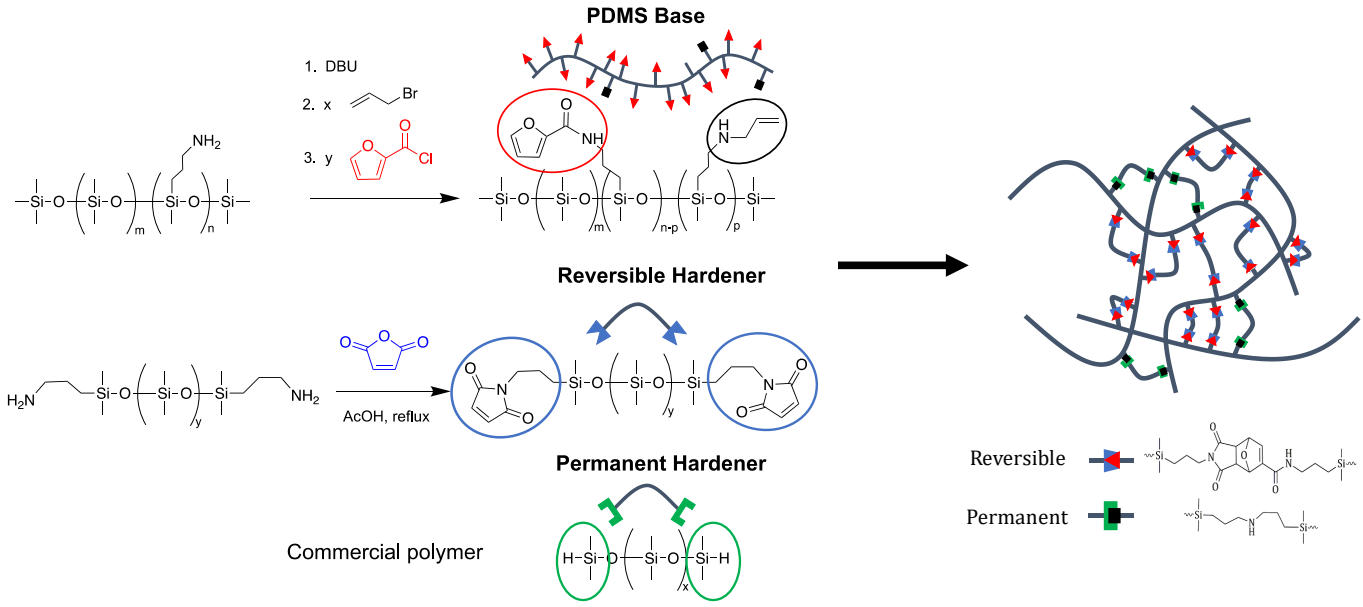


**Scheme 1.** Syntheses of PDMS-base, PDMS-reversible hardener and PDMS double networks

$^1$H NMR analyses were performed on these polymers (Figure S1) to determine their percentage of functionalization. As an example, the $^1$H NMR spectrum of the PDMS functionalized with targeted 10 % allyl groups and 90 % of furan moieties is presented in Figure 1. The $CH_2$ of the PDMS' aliphatic pendant chains at 0.57 ppm was integrated for 200 H. The integrations of the protons' peaks at 4.2 ppm, 5.2 ppm and 5.85 ppm belonging to the allyl moieties integrate for 15.5, 8.8 and 7.3 H, respectively, showing that around 8 % of the pendant amines were allylated. This shows that around 80 % of the allyl bromide initially introduced in the Schlenk were converted. During the second step, a peak at 8.5 ppm corresponding to the proton of the newly formed amide can be observed, as well as the characteristic peaks of the furan moieties at 6.4, 7.1 and 7.41 ppm, showing about 86 % functionalization of the initial PDMS $NH_2$ groups. The compositions of each modified PDMS are given in Table 1 and are in good agreement with targeted values for contents in allyl and furan groups below 30 % and 70 %, respectively. One

can note that the efficiency of the allylation reaction is decreased when a high allyl content is targeted. A value of 62 % was obtained when 75 % of allyl groups were expected. As a result, unreacted free amines remain in this system and are visible at 3 ppm on the $^{1}$H NMR spectrum.

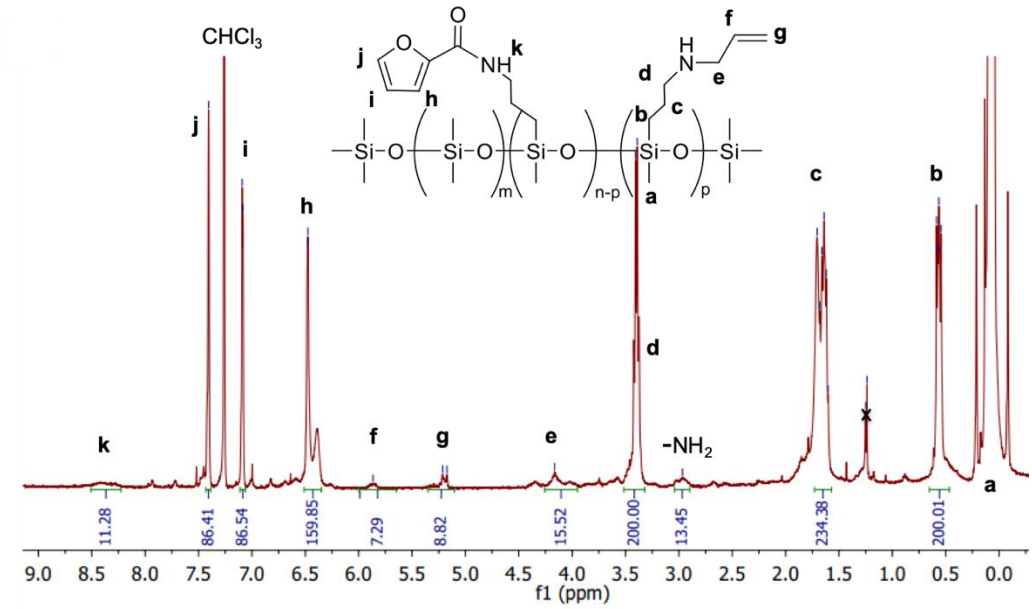


**Figure 1.** $^{1}$H NMR spectrum of PDMS-Furan$_{0.86}$-Allyl$_{0.08}$ in $CDCl_3$

**Table 1.** Preparation of various PDMS bases bearing different amounts of allyl and furan moieties and their corresponding network characteristics

| **Linear functionalized PDMS** | | | | **PDMS networks** | |
|---|---|---|---|---|---|
| **Allyl content** | | **Furan content** | | | |
| **Theor. (%)** | **Exp.[a] (%)** | **Theor. (%)** | **Exp.[a] (%)** | **Swelling ratio[b]** | **Insoluble fraction[c]** |
| 0 | **0** | 100 | **91** | 3.25 ± 0.27 | 0.91 ± 0.01 |
| 10 | **8** | 90 | **86** | 2.76 ± 0.13 | 0.80 ± 0.02 |
| 20 | **20** | 80 | **80** | 2.89 ± 0.15 | 0.88 ± 0.06 |
| 30 | **28** | 70 | **70** | 2.42 ± 0.07 | 0.80 ± 0.06 |
| 75 | **62** | 25 | **18** | 5.90 ± 0.32 | 0.64 ± 0.03 |
| MAPSIL®QS1123 (0% furan) | | | | 1.45 ± 0.03 | 0.98 ± 0.01 |

a) calculated by $^{1}$H NMR spectroscopy; b) calculated from Equation 1, c) calculated from Equation 2

The successful incorporation of allyl and furan moieties on the PDMS base was also confirmed by FTIR-ATR experiments (Figure 2). The peak corresponding to the N-H scissoring δ (N-H) of the amide group can be observed at 1528 $cm^{-1}$. This peak decreases when the amount of allyl functions increases from 0 to 100 %. This tendency was also confirmed with the amide asymmetric stretching $\nu_{as.}$ (C=O) at 1650 $cm^{-1}$.

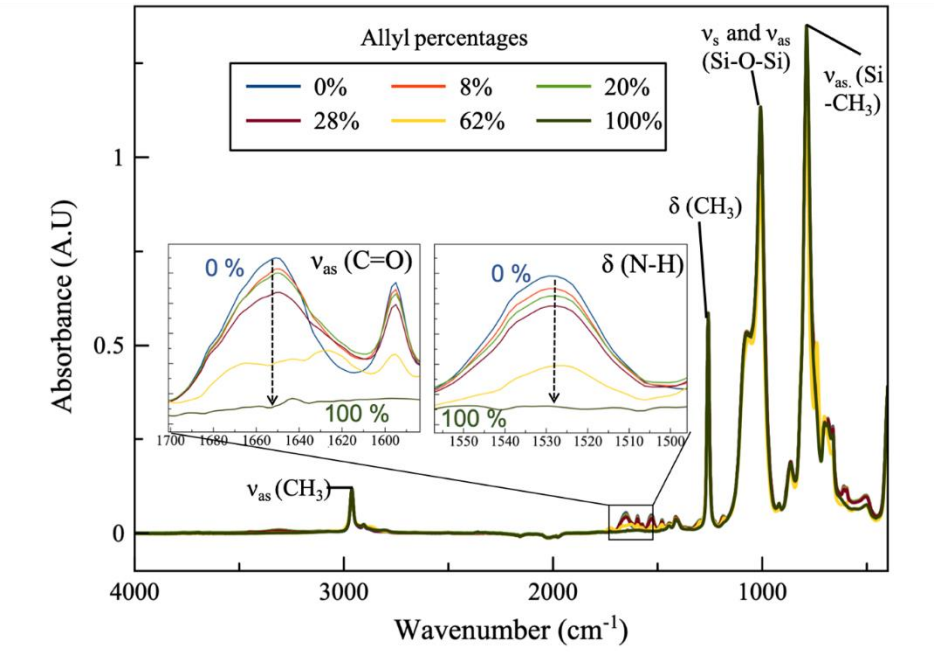


**Figure 2.** Normalized FTIR-ATR spectra of PDMS bases with various amounts of allyl and furan groups used for the elaboration of self-healing materials

In parallel, a telechelic maleimide hardener was synthesized as reversible hardener by reacting an $NH_2$-terminated PDMS with maleic anhydride (Figure S2). The cross-linking of the PDMS bases was performed in the presence of both the reversible hardener and a permanent hardener consisting in a Si-H terminated PDMS. During this step, a Diels-Alder reaction as well as a hydrosilylation in presence of a Karstedt's catalyst occurred. The formation of the permanent network by hydrosilylation and the reversible one by DA reaction was demonstrated by FTIR. As an example, the FTIR spectra of two cross-linked materials with 8 and 20 % allyl contents

are displayed in Figure 3. After cross-linking, the disappearance of the peaks at 910 $cm^{-1}$ and 2125 $cm^{-1}$ (enlargements A & C), corresponding to the Si-H of the permanent hardener (PDMS-H), was observed. The DA reaction can also be demonstrated by the presence of a peak at 1777 $cm^{-1}$ (enlargement B) corresponding to the DA adduct[59].

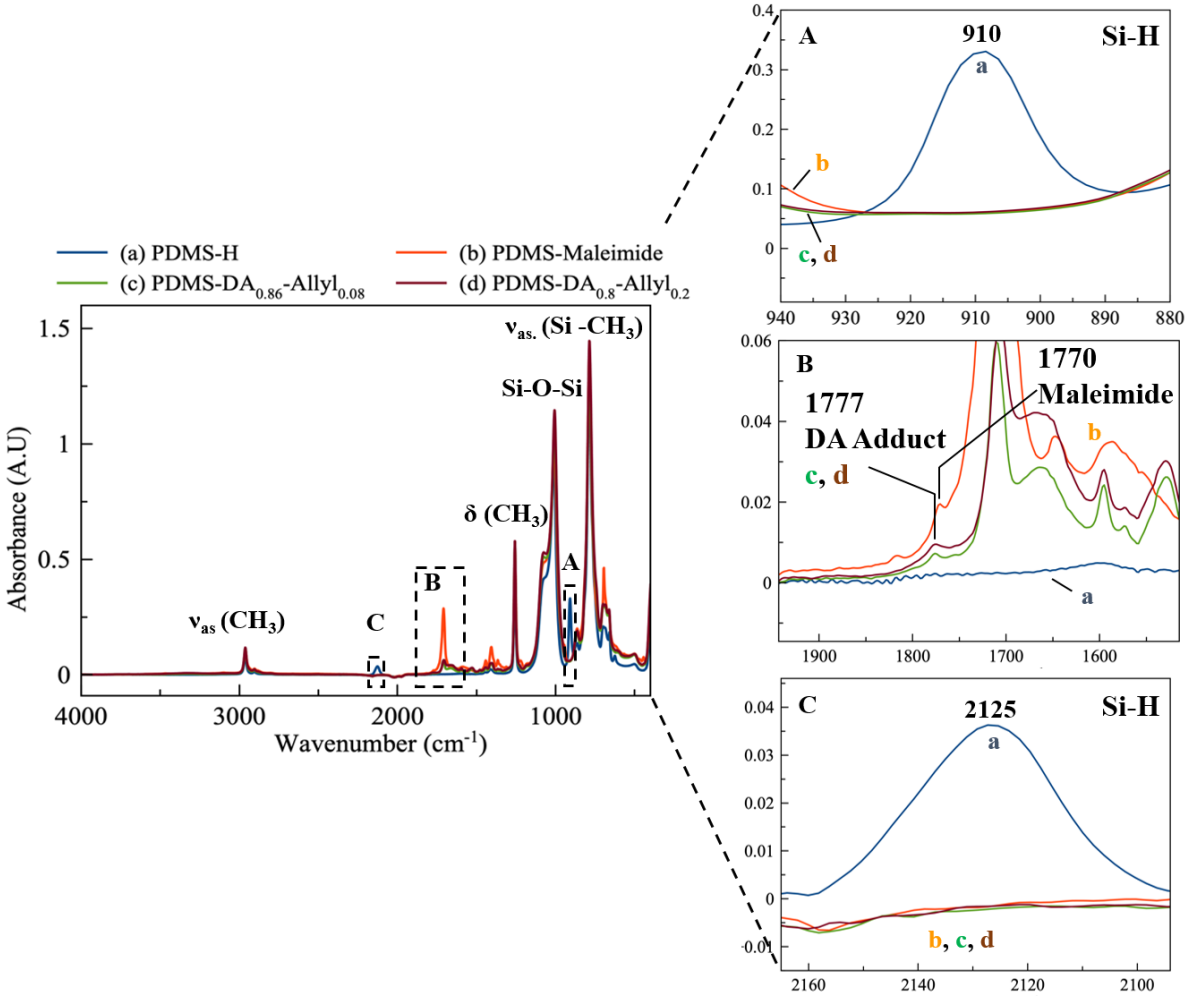


**Figure 3.** Normalized FTIR-ATR spectra of PDMS hardeners and cross-linked materials with enlargements on Si-H peaks (A & C) and on DA adduct peak (B).

Solubility and swelling tests of cross-linked materials were carried out on three replicates and their averages are shown in Table 1. The swelling ratios ranged from 2.4 to 3.3. Insoluble fractions ranging from 80 % to 91 % were obtained for networks synthesized from the PDMS bases contents in allyl functions below 30 %. Such values indicate the occurring of the cross-

linking reactions. As the full cross-linking density is supposed to be constant when allyl and furan parts are added, a constant swelling ratio should be observed. However, for the sample with 62 % of allyl groups (instead of 75 % targeted), the soluble part and swelling ratio were high as compared to other networks. The insoluble fraction decreased with the expected high percentage of permanent network, probably due to the presence of unreacted primary amines, as highlighted before, which are known to poison platinum catalyst[60].

DSC analyses were performed to characterize the elastomers. All of them displayed a low glass transition temperature (Tg) around -120 °C (Figure S3) showing neglectable effect of the introduced organic moieties. Furthermore, the sample cross-linked solely with DA adducts presented a distinguishable endothermic peak at 140 °C corresponding to the retro Diels-Alder reaction as shown by Zhao *et al.* (Figures S3, S4)[31]. This endothermic peak is observed with lower intensity in the case of samples featuring a double network, due to the lower quantity of furan and maleimide functions present in those PDMS (~ 7 %). The integration of rDA peaks decreased when the amount of allyl groups increased because of the lower amount of furan and maleimide moieties. A linear tendancy was obtained between the integrated heat flow of rDA peaks and the amount of moieties responsible of DA reactions (Figure 4). These results confirmed the good incorporation of maleimide in PDMS and therefore the existence of DA network.

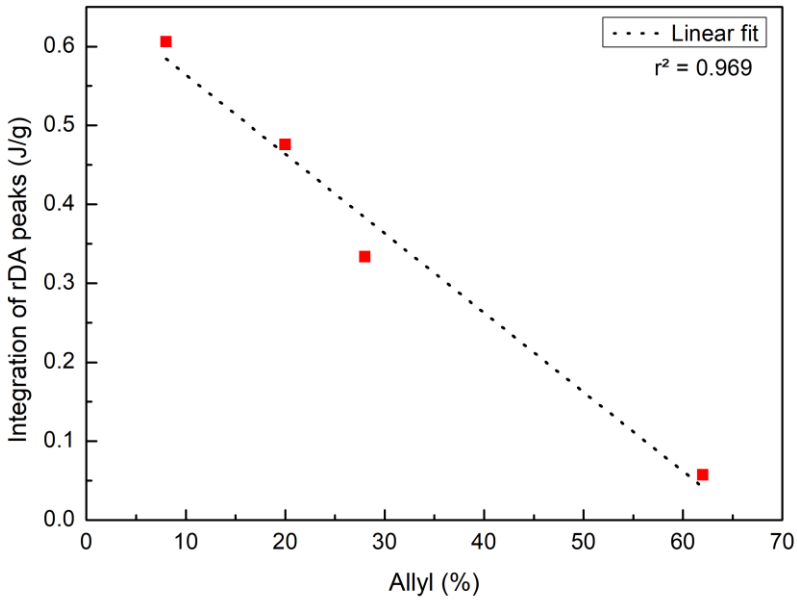


**Figure 4.** Integration of rDA peaks as a function of allyl percentages in PDMS-$DA_x$-$Allyl_y$

Dynamic mechanical analysis of PDMS-$DA_1$-$Allyl_0$ showed a stable elastic modulus (E' = 7.0 $10^4$ Pa) and loss modulus E'' from 25 °C to 100 °C (Figure 5). The small increase of E' around 80 °C is due to the DA reaction between unreacted furan and maleimide functions. Noticeably, E'' increased at 115 °C in agreement with the rDA reaction happening and the flowing of the material, which impeded the analysis to be continued at higher temperature. DMA of PDMS-$DA_{0.86}Allyl_{0.08}$ showed a different behavior (Figure 5). With the addition of the allyl part, and therefore of a permanent network, the rDA was not observed. Contrary to PDMS-$DA_1$-$Allyl_0$, E'' remained constant from 0 °C to 200 °C meaning that rDA does not affect the mechanical properties of the material. Thus, the presence of the permanent network through hydrosilylation maintained the mechanical properties of the polymer even if the dynamic network is broken. One can note a slight increase of the elastic modulus for PDMS-$DA_{0.86}Allyl_{0.08}$ above 140 °C, which can be attributed to a secondary cross-linking and discussed below.

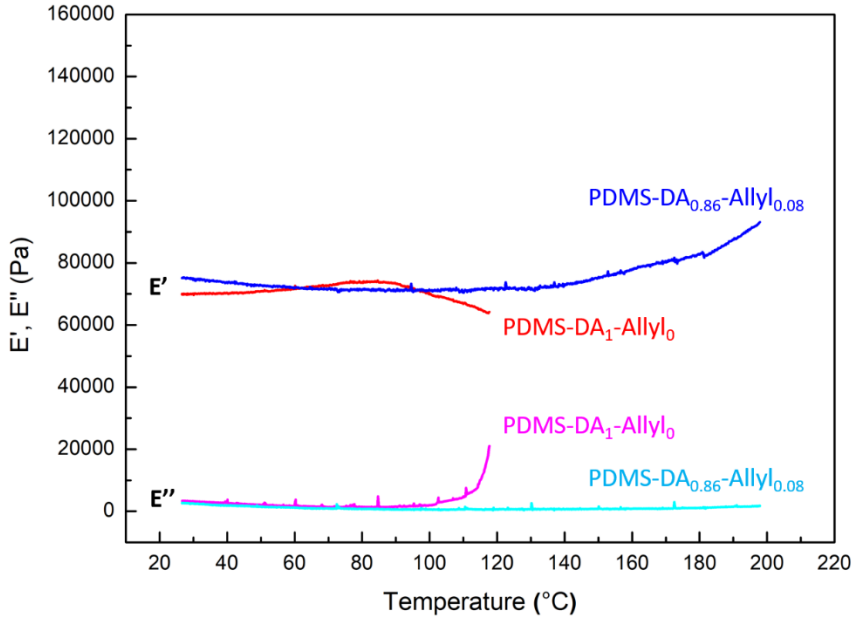


**Figure 5.** DMA analyses of PDMS-$DA_1$-$Allyl_0$ (red & pink) and PDMS-$DA_{0.86}$-$Allyl_{0.08}$ (blue & cyan)

To demonstrate qualitatively their self-healing ability, modified PDMS underwent in a first time a scratch-healing test in which the evaluation of the damaged surface was carried out by optical microscopy. As shown in Figure 6A, the cuts were repaired partially after 48 hours at 70 °C. In a second time, PDMS materials underwent a remolding test in which they were cut into small pieces and placed into a mold at 140 °C under mechanical pressure for 1 hour, allowing DA cyclo-adducts to break. They were then left at 70 °C for 48 hours in an oven to reform the adducts and maximize the recovery of mechanical properties (Figure 6B).

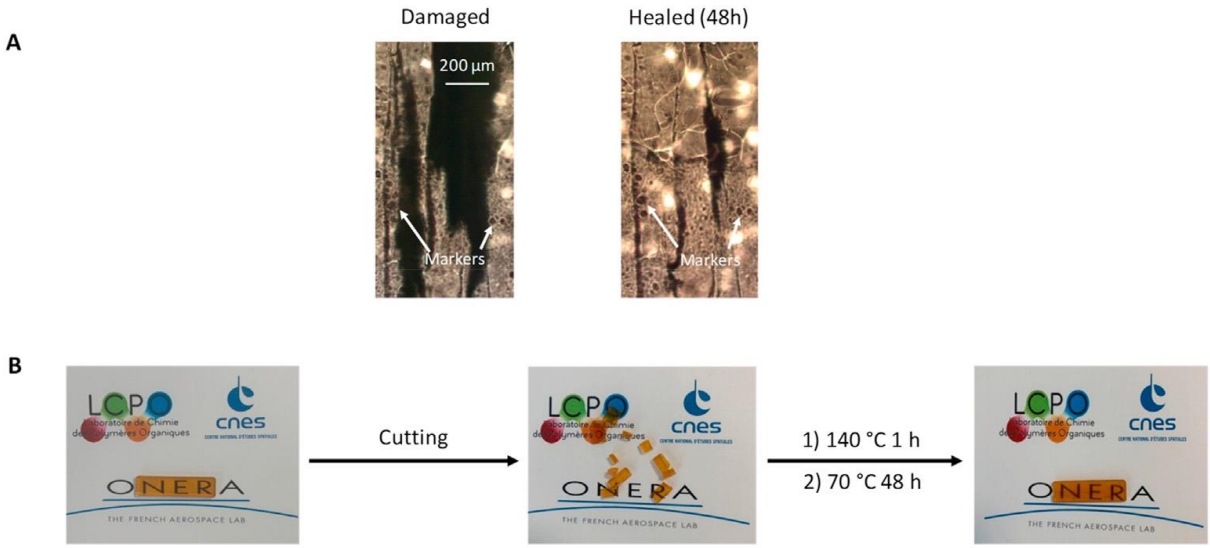


**Figure 6.** Self-healing ability of a modified PDMS: A) evaluated by optical microscopy after a scratch test (sample shown is PDMS-$DA_{0.7}$-$Allyl_{0.28}$) and B) by remolding process (sample shown is PDMS-$DA_{0.8}$-$Allyl_{0.2}$)

Tensile strength analyses were then performed on the pristine and healed PDMS-$DA_{0.8}$-$Allyl_{0.2}$ material used as a model system (Figure 7A). The pristine sample exhibited an elongation at break of 113 %, a stress at break of 25 kPa and an elastic modulus equal to $5.2x10^4$ Pa. The sample was then cut into pieces and healed at 140 °C before performing the same test. This sequence was repeated twice. The elongation at break obtained was 40 % for the first healing and 30 % after the second healing. The stress at break and elastic modulus increased significantly after healing, up to 112 kPa and $3.3x10^5$ Pa, respectively, allowing the assumption that the cross-linking degree was higher after the healing procedure probably due to a secondary cross-linking reaction during the thermal treatment above 140 °C. This phenomenon was investigated by DSC. The thermogram of the PDMS-$DA_0$-$Allyl_1$ (Figure S5a) displayed an exothermic peak starting at 147 °C. A similar peak starting at 139 °C was observed on the DSC of the MAPSIL® QS1123 reference, containing only vinyl-PDMS and H-branched PDMS (Figure S5b). This secondary cross-linking reaction corresponds to a hydrosilylation from residual H-terminated PDMS and residual alkene from PDMS "Base". This observation is in

agreement with the increase of the elastic modulus observed in the DMA of PDMS-$DA_{0.86}Allyl_{0.08}$ (Figure 5). To avoid these secondary cross-linkings, some materials were thermally treated at 160 °C for 1 hour before performing tensile strength analyses. The stress at break and elastic modulus were shown higher than the pristine material without heat treatment (Figure 7B). Similar elastic moduli were obtained before and after healing. One can note that strain or stress at break are a bit different but are in the same range as shown in Table 2. This heat treatment seems to fully cross-link the materials without observing a secondary reaction.

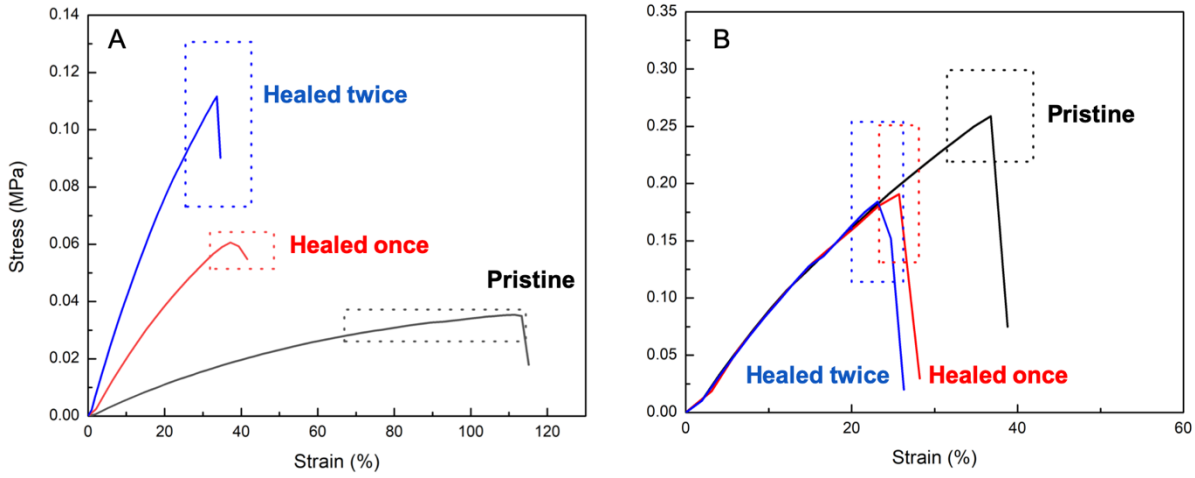


**Figure 7.** Tensile stress *vs* strain plots of PDMS-$DA_{0.8}$-$Allyl_{0.2}$ depending on the number of healings: A) before heat treatment, B) after heat treatment (Standard deviation calculated on 7 to 8 samples are represented by dashed rectangles)

**Table 2.** Elastic modulus, stress and strain of PDMS-$DA_{0.8}$-$Allyl_{0.2}$ before and after heat treatment.

| | PDMS-$DA_{0.8}$-$Allyl_{0.2}$ | Elastic Modulus (MPa) | Stress (MPa) | Strain (%) |
|---|---|---|---|---|
| **Before heat treatment** | **Pristine** | 0.0597±0.008 | 0.0316±0.006 | 91±24 |
| | **Healed once** | 0.192±0.024 | 0.0580±0.006 | 40±8 |
| | **Healed twice** | 0.367±0.071 | 0.102±0.03 | 34±9 |
| **After heat treatment** | **Pristine** | 0.817±0.020 | 0.259±0.04 | 37±5 |
| | **Healed once** | 0.804±0.037 | 0.191±0.06 | 26±2 |
| | **Healed twice** | 0.810±0.027 | 0.184±0.07 | 23±3 |

Samples were finally irradiated in the SEMIRAMIS vacuum chamber linked to a 2.5 MeV Van de Graaf proton accelerator generating proton with an energy of 240 keV. Each sample was doubled in the sample holder to confirm the result of proton irradiation and to avoid effects due to proton flux inhomogeneity in the facility. These irradiations induce rearrangement in the molecular structure due to the formation of radical species[61]. For most samples, cracks appeared as shown in Figure 8. MAPSIL® QS1123, used as reference and characterized by a fully permanent network, was the most cracked sample. PDMS-$DA_1$-$Allyl_0$ used as the reference for full reversible Diels-Alder network also cracked but less than the MAPSIL® QS1123 as the number of cracks per unit area was shown to be lower. Similar observations could be made for PDMS-$DA_{0.86}$-$Allyl_{0.08}$ and PDMS-$DA_{0.8}$-$Allyl_{0.2}$. Interestingly, the amount of cracks was shown to decrease even more for PDMS-$DA_{0.7}$-$Allyl_{0.28}$ when increasing the amount of permanent network, and to disappear for PDMS-$DA_{0.18}$-$Allyl_{0.62}$ despite the low amount of DA network. DA cycloadducts are assumed to dissociate into furan and maleimide moieties under proton irradiation since the bond strength of DA adduct is lower than other covalent bonds[37]. The collision of incident protons of 240 keV with the material could locally give the requested energy to disrupt and reform DA cycloadduct and will be discussed below. The blocked structure of the network through covalent bonding promotes structural integrity and would bring furan and maleimide moieties closer to reform DA cycloadducts allowing self-healing. In another system, Sumerlin abd co-workers proved the symbiosis of static and reversible networks to get a good balance in terms of self-healing and mechanical properties[62].

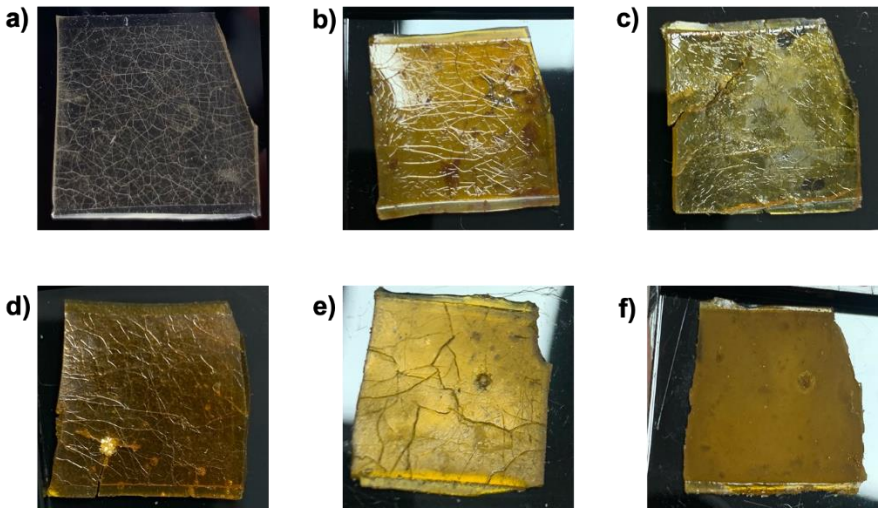


**Figure 8.** Pictures of materials after proton irradiation: a) MAPSIL®QS1123 b) PDMS-$DA_1$-$Allyl_0$ c) PDMS-$DA_{0.86}$-$Allyl_{0.08}$ d) PDMS-$DA_{0.8}$-$Allyl_{0.2}$ e) PDMS-$DA_{0.7}$-$Allyl_{0.28}$ f) PDMS-$DA_{0.18}$-$Allyl_{0.62}$

UV-Vis-NIR spectroscopy was carried out on polymeric films before and after irradiation (Figure S6). Samples were place on mirrors to record their reflectance ($R_{S+M}$) spectra using an integrating sphere. The systematic drop in reflectance at 800 nm corresponds to an artefact due to the mirror system. The main differences before and after irradiation were present in the UV-Vis region. MAPSIL® QS1123 exhibited a bathochromic shift due to the formation of absorbing species. No major change was seen for PDMS-$DA_x$-$Allyl_y$, aside from a small reflectance drop, proving the conservation of optical properties, useful for coating applications.

In order to correlate the crack density observed on the pictures and the chemical structure of the networks, FTIR-ATR analyses of materials before and after irradiation were also performed (Figure 9). The absorbance of all peaks dropped down, and the apparition of new peaks was noticed between 3500 and 3000 $cm^{-1}$ for simple networks (MAPSIL®QS1123 and PDMS-$DA_1$-$Allyl_0$). Based on a literature report[63], this large peak was attributed to the Si-OH stretching coming from the rupture of Si-O backbone since the experiment takes place in high vacuum environment, without oxygen. The apparition of broad peaks at 1625 $cm^{-1}$ corresponding to C=C stretching indicated the formation of alkene functions as shown in Scheme 2. After

irradiation, the absorbance of the peaks corresponding to the C=O bonds at 1710 $cm^{-1}$ belonging to the DA units and to the $CH_3$ deformation at 1260 $cm^{-1}$ corresponding to PDMS backbone showed a continuous decrease when increasing the amount of DA network. Interstingly, a low degradation was obtained for double networks with low amount of reversible moieties and high amount of permanent ones. A specific peak for DA adducts was observed at 1777 $cm^{-1}$ for all PDMS materials based on double networks before irradiation (Figure 9A). This same peak was observed after irradiation only for PDMS-$DA_{0.8}$-$Allyl_{0.2}$, PDMS-$DA_{0.7}$-$Allyl_{0.28}$ and PDMS-$DA_{0.18}$-$Allyl_{0.68}$ showing that DA adducts are still present in these materials (Figure 9B). A synergistic effect of the double network toward ageing was observed as simple networks were the most deteriorated. It is consistent with the hypothesis previously made: the permanent network maintains the 3D network conformation to facilitate self-healing. Furthermore, samples showing less cracks (PDMS-$DA_{0.7}$-$Allyl_{0.28}$ & PDMS-$DA_{0.18}$-$Allyl_{0.62}$) are also less degraded, according to FTIR analyses. Thus, the presence of the double network incorporated in PDMS showed a better stability upon proton irradiations than single networks. Based on these main results, namely the reduction of the amount of cracks (up to their disappearance), the lower chemical degradation and the presence of DA adducts after irradiation, it seems that a double network consisting of a high percentage of permanent network and a low percentage of reversible one is the good balance to enhance ageing properties under proton irradiation while preserving good mechanical properties.

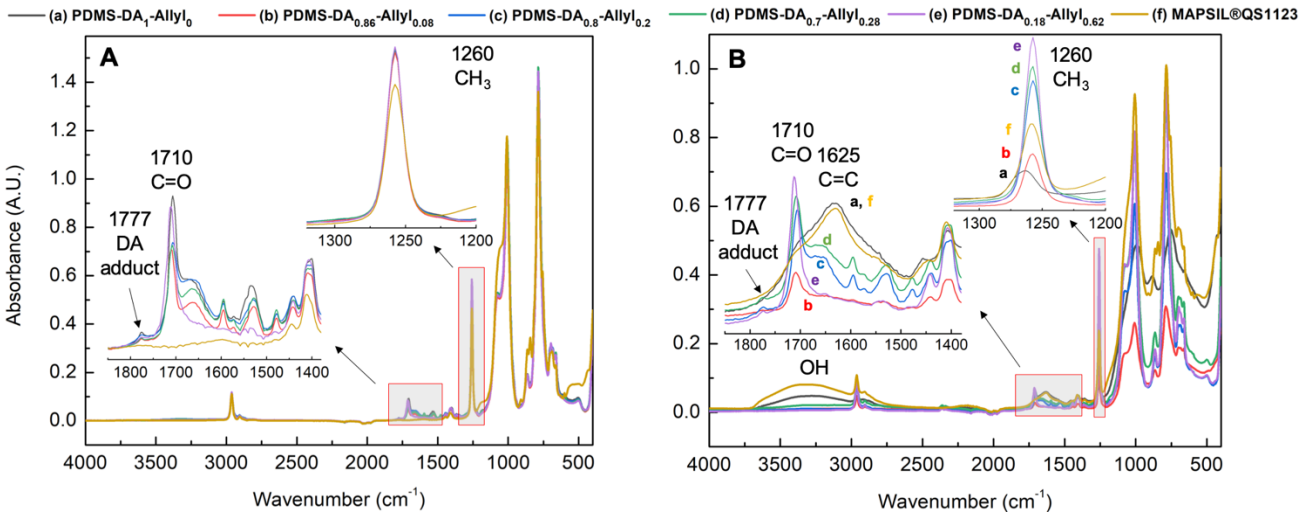


**Figure 9.** FTIR-ATR spectra of PDMS-DA$_x$-Ally$_y$ and MAPSIL® QS1123 A) before and B) after proton irradiation

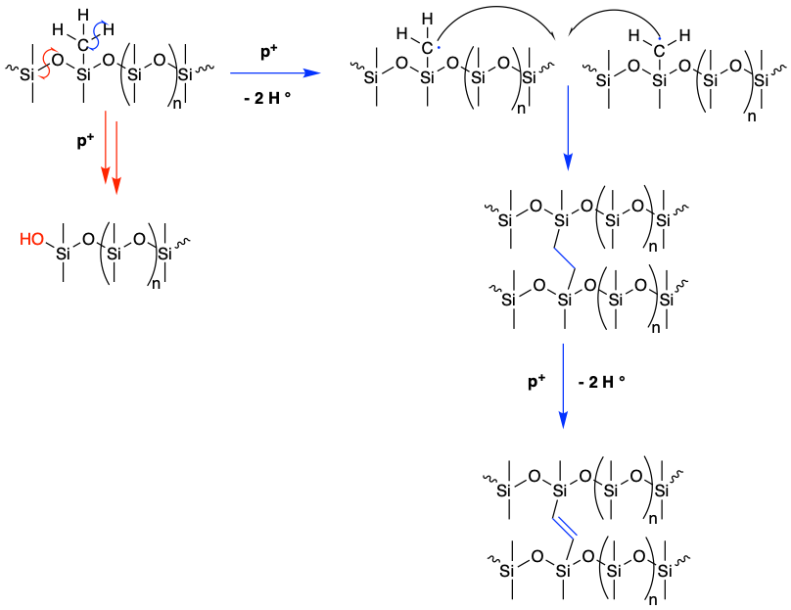


**Scheme 2.** Proposed rearrangements of PDMS after proton irradiation

## 4. Conclusion

A route to prepare self-healing PDMS materials was elaborated from commercial polymers. Bases featuring different ratios of furan and allyl groups were synthesized by a two-step procedure. A reversible hardener bearing maleimide functions was also prepared. Cross-linking

of material was carried out by mixing the base, the reversible hardener and the permanent hardener allowing the formation of a double network by both Diels-Alder and hydrosilylation reactions. The rDA reaction was shown to occur at around 140 °C. With the incorporation of the permanent network through hydrosilylation, flowing of the material was not observed during DMA experiments, thus maintaining expected PDMS mechanical properties. Regarding ageing properties under proton irradiation, materials with double networks, and in particular those with high allyl contents, exhibited fewer to no cracks. To summarize, the addition of permanent cross-links allows the materials to self-heal while remaining cohesive even when the DA network breaks, thus resolving a main issue of full DA systems in the self-healing field.

## Declaration of competing interest

The authors declare that they have no known competing financial interests or personal relationships that could have appeared to influence the work reported in this paper.

## CRediT authorship contribution statement

**Dijwar Yilmaz:** Writing- original draft, Investigation, Conceptualization, Visualization, Methodology. **David Lansade:** Writing - review & editing, Investigation, Conceptualization, Visualization, Methodology. **Simon Lewandowski:** Writing - review & editing, Visualization, Supervision, Project administration, Conceptualization, Methodology. **Sophie Perraud:** Conceptualization, Resources, Project administration. **Audrey Llevot:** Writing - review & editing, Visualization, Supervision, Conceptualization, Methodology **Stéphane Carlotti:** Writing - review & editing, Visualization, Supervision, Project administration, Conceptualization, Methodology.

## Acknowledgments

This work was supported by a cofunding between Centre National d'Etudes Spatiales, the French Space Agency, and ONERA, the French Aerospace Lab. The authors would like to thank Claude Pons and Romain Rey from ONERA Toulouse Center for running proton irradiation experiments.

## References:

(1) Planes, M.; Le Coz, C.; Soum, A.; Carlotti, S.; Rejsek-Riba, V.; Lewandowski, S.; Remaury, S.; Solé, S. Polydimethylsiloxane/Additive Systems for Thermal and Ultraviolet Stability in Geostationary Environment. *J. Spacecr. Rockets* **2016**, *53* (6), 1128–1133. https://doi.org/10.2514/1.A33484.

(2) Stanton, M. M.; Ducker, R. E.; MacDonald, J. C.; Lambert, C. R.; Grant McGimpsey, W. Super-Hydrophobic, Highly Adhesive, Polydimethylsiloxane (PDMS) Surfaces. *J. Colloid Interface Sci.* **2012**, *367* (1), 502–508. https://doi.org/10.1016/j.jcis.2011.07.053.

(3) Lee, B. K.; Ryu, J. H.; Baek, I.-B.; Kim, Y.; Jang, W. I.; Kim, S.-H.; Yoon, Y. S.; Kim, S. H.; Hong, S.-G.; Byun, S.; Yu, H. Y. Silicone-Based Adhesives with Highly Tunable Adhesion Force for Skin-Contact Applications. *Adv. Healthc. Mater.* **2017**, *6* (22), 1700621. https://doi.org/10.1002/adhm.201700621.

(4) Lansade, D.; Lewandowski, S.; Remaury, S.; Sierra, G.; Solé, S.; Perraud, S.; Carlotti, S. Enhanced Resistance to Proton Irradiation of Poly(Dimethylsiloxane) Resins through Surface Embedding of Silica Photonic Crystals. *Polym. Degrad. Stab.* **2020**, *176*, 109163. https://doi.org/10.1016/j.polymdegradstab.2020.109163.

(5) Planes, M.; Brand, J.; Lewandowski, S.; Remaury, S.; Solé, S.; Le Coz, C.; Carlotti, S.; Sèbe, G. Improvement of the Thermal and Optical Performances of Protective Polydimethylsiloxane Space Coatings with Cellulose Nanocrystal Additives. *ACS Appl. Mater. Interfaces* **2016**, *8* (41), 28030–28039. https://doi.org/10.1021/acsami.6b09043.

(6) Zhang, Y.; Zheng, J.; Fang, C.; Li, Z.; Zhao, X.; Li, Y.; Ruan, X.; Dai, Y. Enhancement of Silicon-Wafer Solar Cell Efficiency with Low-Cost Wrinkle Antireflection Coating of Polydimethylsiloxane. *Sol. Energy Mater. Sol. Cells* **2018**, *181*, 15–20. https://doi.org/10.1016/j.solmat.2017.10.004.

(7) Mata, A.; Fleischman, A. J.; Roy, S. Characterization of Polydimethylsiloxane (PDMS) Properties for Biomedical Micro/Nanosystems. *Biomed. Microdevices* **2005**, *7* (4), 281–293. https://doi.org/10.1007/s10544-005-6070-2.

(8) Fujii, T. PDMS-Based Microfluidic Devices for Biomedical Applications. *Microelectron. Eng.* **2002**, *61–62*, 907–914. https://doi.org/10.1016/S0167-9317(02)00494-X.

(9) Raj M, K.; Chakraborty, S. PDMS Microfluidics: A Mini Review. *J. Appl. Polym. Sci.* **2020**, *137* (27), 48958. https://doi.org/10.1002/app.48958.

(10) Friend, J.; Yeo, L. Fabrication of Microfluidic Devices Using Polydimethylsiloxane. *Biomicrofluidics* **2010**, *4* (2), 026502. https://doi.org/10.1063/1.3259624.

(11) Hassanpour-Tamrin, S.; Sanati-Nezhad, A.; Sen, A. A Simple and Low-Cost Approach for Irreversible Bonding of Polymethylmethacrylate and Polydimethylsiloxane at Room Temperature for High-Pressure Hybrid Microfluidics. *Sci. Rep.* **2021**, *11* (1), 4821. https://doi.org/10.1038/s41598-021-83011-8.
(12) Xiao, H.; Li, C.; Yang, D.; Li, X.; He, S. Optical Degradation of Polydimethylsiloxane under 150 KeV Proton Exposure. *J. Appl. Polym. Sci.* **2008**, *109* (6), 4060–4064. https://doi.org/10.1002/app.28591.
(13) Stevenson, I.; David, L.; Gauthier, C.; Arambourg, L.; Davenas, J.; Vigier, G. Influence of SiO2 Fillers on the Irradiation Ageing of Silicone Rubbers. *Polymer* **2001**, *42* (22), 9287–9292. https://doi.org/10.1016/S0032-3861(01)00470-0.
(14) Di, M.; He, S.; Li, R.; Yang, D. Resistance to Proton Radiation of Nano-TiO2 Modified Silicone Rubber. *Nucl. Instrum. Methods Phys. Res. Sect. B Beam Interact. Mater. At.* **2006**, *252* (2), 212–218. https://doi.org/10.1016/j.nimb.2006.08.008.
(15) Cho, S. H.; Andersson, H. M.; White, S. R.; Sottos, N. R.; Braun, P. V. Polydimethylsiloxane-Based Self-Healing Materials. *Adv. Mater.* **2006**, *18* (8), 997–1000. https://doi.org/10.1002/adma.200501814.
(16) Simonin, L.; Falco, G.; Pensec, S.; Dalmas, F.; Chenal, J.-M.; Ganachaud, F.; Marcellan, A.; Chazeau, L.; Bouteiller, L. Macromolecular Additives to Turn a Thermoplastic Elastomer into a Self-Healing Material. *Macromolecules* **2021**, *54* (2), 888–895. https://doi.org/10.1021/acs.macromol.0c02352.
(17) Sun, F.; Xu, J.; Liu, T.; Li, F.; Poo, Y.; Zhang, Y.; Xiong, R.; Huang, C.; Fu, J. An Autonomously Ultrafast Self-Healing, Highly Colourless, Tear-Resistant and Compliant Elastomer Tailored for Transparent Electromagnetic Interference Shielding Films Integrated in Flexible and Optical Electronics. *Mater. Horiz.* **2021**. https://doi.org/10.1039/D1MH01199E.
(18) Mei, J.-F.; Jia, X.-Y.; Lai, J.-C.; Sun, Y.; Li, C.-H.; Wu, J.-H.; Cao, Y.; You, X.-Z.; Bao, Z. A Highly Stretchable and Autonomous Self-Healing Polymer Based on Combination of Pt···Pt and π-π Interactions. *Macromol. Rapid Commun.* **2016**, *37* (20), 1667–1675. https://doi.org/10.1002/marc.201600428.
(19) Li, C.-H.; Wang, C.; Keplinger, C.; Zuo, J.-L.; Jin, L.; Sun, Y.; Zheng, P.; Cao, Y.; Lissel, F.; Linder, C.; You, X.-Z.; Bao, Z. A Highly Stretchable Autonomous Self-Healing Elastomer. *Nat. Chem.* **2016**, *8* (6), 618–624. https://doi.org/10.1038/nchem.2492.
(20) Tan, H.; Lyu, Q.; Xie, Z.; Li, M.; Wang, K.; Wang, K.; Xiong, B.; Zhang, L.; Zhu, J. Metallosupramolecular Photonic Elastomers with Self-Healing Capability and Angle-Independent Color. *Adv. Mater.* **2018**, 1805496. https://doi.org/10.1002/adma.201805496.
(21) Rao, Y.-L.; Chortos, A.; Pfattner, R.; Lissel, F.; Chiu, Y.-C.; Feig, V.; Xu, J.; Kurosawa, T.; Gu, X.; Wang, C.; He, M.; Chung, J. W.; Bao, Z. Stretchable Self-Healing Polymeric Dielectrics Cross-Linked Through Metal–Ligand Coordination. *J. Am. Chem. Soc.* **2016**, *138* (18), 6020–6027. https://doi.org/10.1021/jacs.6b02428.
(22) Arslan, M.; Kiskan, B.; Yagci, Y. Benzoxazine-Based Thermoset with Autonomous Self-Healing and Shape Recovery. *Macromolecules* **2018**, *51* (24), 10095–10103. https://doi.org/10.1021/acs.macromol.8b02137.
(23) Sinawang, G.; Osaki, M.; Takashima, Y.; Yamaguchi, H.; Harada, A. Supramolecular Self-Healing Materials from Non-Covalent Cross-Linking Host–guest Interactions. *Chem. Commun.* **2020**, *56* (32), 4381–4395. https://doi.org/10.1039/D0CC00672F.
(24) Madsen, F. B.; Yu, L.; Skov, A. L. Self-Healing, High-Permittivity Silicone Dielectric Elastomer. *ACS Macro Lett.* **2016**, *5* (11), 1196–1200. https://doi.org/10.1021/acsmacrolett.6b00662.
(25) Aguirresarobe, R. H.; Martin, L.; Fernandez-Berridi, M. J.; Irusta, L. Autonomic Healable Waterborne Organic-Inorganic Polyurethane Hybrids Based on Aromatic Disulfide Moieties. *Express Polym. Lett.* **2017**, *11* (4), 266–277. https://doi.org/10.3144/expresspolymlett.2017.27.

(26) Rekondo, A.; Martin, R.; Ruiz de Luzuriaga, A.; Cabañero, G.; Grande, H. J.; Odriozola, I. Catalyst-Free Room-Temperature Self-Healing Elastomers Based on Aromatic Disulfide Metathesis. *Mater Horiz* **2014**, *1* (2), 237–240. https://doi.org/10.1039/C3MH00061C.
(27) Arslan, M.; Kiskan, B.; Yagci, Y. Recycling and Self-Healing of Polybenzoxazines with Dynamic Sulfide Linkages. *Sci. Rep.* **2017**, *7* (1), 5207. https://doi.org/10.1038/s41598-017-05608-2.
(28) Zhang, B.; Zhang, P.; Zhang, H.; Yan, C.; Zheng, Z.; Wu, B.; Yu, Y. A Transparent, Highly Stretchable, Autonomous Self-Healing Poly(Dimethyl Siloxane) Elastomer. *Macromol. Rapid Commun.* **2017**, *38* (15), 1700110. https://doi.org/10.1002/marc.201700110.
(29) Wang, P.; Yang, L.; Dai, B.; Yang, Z.; Guo, S.; Gao, G.; Xu, L.; Sun, M.; Yao, K.; Zhu, J. A Self-Healing Transparent Polydimethylsiloxane Elastomer Based on Imine Bonds. *Eur. Polym. J.* **2020**, *123*, 109382. https://doi.org/10.1016/j.eurpolymj.2019.109382.
(30) Lei, X.; Huang, Y.; Liang, S.; Zhao, X.; Liu, L. Preparation of Highly Transparent, Room-Temperature Self-Healing and Recyclable Silicon Elastomers Based on Dynamic Imine Bond and Their Ion Responsive Properties. *Mater. Lett.* **2020**, *268*, 127598. https://doi.org/10.1016/j.matlet.2020.127598.
(31) Wang, Z.; Gangarapu, S.; Escorihuela, J.; Fei, G.; Zuilhof, H.; Xia, H. Dynamic Covalent Urea Bonds and Their Potential for Development of Self-Healing Polymer Materials. *J. Mater. Chem. A* **2019**, *7* (26), 15933–15943. https://doi.org/10.1039/C9TA02054C.
(32) Zhang, Y.; Yuan, L.; Liang, G.; Gu, A. Simultaneously Achieving Superior Foldability, Mechanical Strength and Toughness for Transparent Healable Polysiloxane Films through Building Hierarchical Crosslinked Networks and Dual Dynamic Bonds. *J. Mater. Chem. A* **2018**, *6* (46), 23425–23434. https://doi.org/10.1039/C8TA07580H.
(33) Yan, Q.; Zhao, L.; Cheng, Q.; Zhang, T.; Jiang, B.; Song, Y.; Huang, Y. Self-Healing Polysiloxane Elastomer Based on Integration of Covalent and Reversible Networks. *Ind. Eng. Chem. Res.* **2019**, *58* (47), 21504–21512. https://doi.org/10.1021/acs.iecr.9b04355.
(34) Wang, J.; Lv, C.; Li, Z.; Zheng, J. Facile Preparation of Polydimethylsiloxane Elastomer with Self-Healing Property and Remoldability Based on Diels-Alder Chemistry. *Macromol. Mater. Eng.* **2018**, *303* (6), 1800089. https://doi.org/10.1002/mame.201800089.
(35) Sun, H.; Kabb, C. P.; Dai, Y.; Hill, M. R.; Ghiviriga, I.; Bapat, A. P.; Sumerlin, B. S. Macromolecular Metamorphosis via Stimulus-Induced Transformations of Polymer Architecture. *Nat. Chem.* **2017**, *9* (8), 817–823. https://doi.org/10.1038/nchem.2730.
(36) Engle, L. P.; Wagener, K. B. A Review of Thermally Controlled Covalent Bond Formation in Polymer Chemistry. *J. Macromol. Sci. Part C Polym. Rev.* **1993**, *33* (3), 239–257. https://doi.org/10.1080/15321799308021436.
(37) Chen, X.; Dam, M. A.; Ono, K.; Mal, A.; Shen, H.; Nutt, S. R.; Sheran, K.; Wudl, F. A Thermally Re-Mendable Cross-Linked Polymeric Material. *Science* **2002**, *295* (5560), 1698–1702. https://doi.org/10.1126/science.1065879.
(38) Berto, P.; Pointet, A.; Le Coz, C.; Grelier, S.; Peruch, F. Recyclable Telechelic Cross-Linked Polybutadiene Based on Reversible Diels–Alder Chemistry. *Macromolecules* **2018**, *51* (3), 651–659. https://doi.org/10.1021/acs.macromol.7b02220.
(39) Tanasi, P.; Hernández Santana, M.; Carretero-González, J.; Verdejo, R.; López-Manchado, M. A. Thermo-Reversible Crosslinked Natural Rubber: A Diels-Alder Route for Reuse and Self-Healing Properties in Elastomers. *Polymer* **2019**, *175*, 15–24. https://doi.org/10.1016/j.polymer.2019.04.059.
(40) Bai, J.; Li, H.; Shi, Z.; Yin, J. An Eco-Friendly Scheme for the Cross-Linked Polybutadiene Elastomer via Thiol–Ene and Diels–Alder Click Chemistry. *Macromolecules* **2015**, *48* (11), 3539–3546. https://doi.org/10.1021/acs.macromol.5b00389.
(41) Utrera-Barrios, S.; Verdejo, R.; López-Manchado, M. A.; Hernández Santana, M. Evolution of Self-Healing Elastomers, from Extrinsic to Combined Intrinsic Mechanisms: A Review. *Mater. Horiz.* **2020**, *7* (11), 2882–2902. https://doi.org/10.1039/D0MH00535E.

(42) Jia, Z.; Zhu, S.; Chen, Y.; Zhang, W.; Zhong, B.; Jia, D. Recyclable and Self-Healing Rubber Composites Based on Thermorevesible Dynamic Covalent Bonding. *Compos. Part Appl. Sci. Manuf.* **2020**, *129*, 105709. https://doi.org/10.1016/j.compositesa.2019.105709.
(43) Kuang, X.; Liu, G.; Dong, X.; Wang, D. Enhancement of Mechanical and Self-Healing Performance in Multiwall Carbon Nanotube/Rubber Composites via Diels-Alder Bonding. *Macromol. Mater. Eng.* **2016**, *301* (5), 535–541. https://doi.org/10.1002/mame.201500425.
(44) Trovatti, E.; Lacerda, T. M.; Carvalho, A. J. F.; Gandini, A. Recycling Tires? Reversible Crosslinking of Poly(Butadiene). *Adv. Mater.* **2015**, *27* (13), 2242–2245. https://doi.org/10.1002/adma.201405801.
(45) Behera, P. K.; Mondal, P.; Singha, N. K. Self-Healable and Ultrahydrophobic Polyurethane-POSS Hybrids by Diels–Alder "Click" Reaction: A New Class of Coating Material. *Macromolecules* **2018**, *51* (13), 4770–4781. https://doi.org/10.1021/acs.macromol.8b00583.
(46) Behera, P. K.; Raut, S. K.; Mondal, P.; Sarkar, S.; Singha, N. K. Self-Healable Polyurethane Elastomer Based on Dual Dynamic Covalent Chemistry Using Diels–Alder "Click" and Disulfide Metathesis Reactions. *ACS Appl. Polym. Mater.* **2021**, *3* (2), 847–856. https://doi.org/10.1021/acsapm.0c01179.
(47) Fang, Y.; Du, X.; Yang, S.; Wang, H.; Cheng, X.; Du, Z. Sustainable and Tough Polyurethane Films with Self-Healability and Flame Retardance Enabled by Reversible Chemistry and Cyclotriphosphazene. *Polym. Chem.* **2019**, *10* (30), 4142–4153. https://doi.org/10.1039/C9PY00680J.
(48) Fang, Y.; Li, J.; Du, X.; Du, Z.; Cheng, X.; Wang, H. Thermal- and Mechanical-Responsive Polyurethane Elastomers with Self-Healing, Mechanical-Reinforced, and Thermal-Stable Capabilities. *Polymer* **2018**, *158*, 166–175. https://doi.org/10.1016/j.polymer.2018.10.056.
(49) Feng, L.; Bian, Y.; Chai, C.; Qiang, X. Effect of Heat-Treatment on Self-Healing and Processing Behavior of Thermally Reversible Polyurethanes. *J. Polym. Environ.* **2020**, *28* (2), 647–656. https://doi.org/10.1007/s10924-019-01633-6.
(50) Truong, T. T.; Thai, S. H.; Nguyen, H. T.; Phung, D. T. T.; Nguyen, L. T.; Pham, H. Q.; Nguyen, L.-T. T. Tailoring the Hard–Soft Interface with Dynamic Diels–Alder Linkages in Polyurethanes: Toward Superior Mechanical Properties and Healability at Mild Temperature. *Chem. Mater.* **2019**, *31* (7), 2347–2357. https://doi.org/10.1021/acs.chemmater.8b04624.
(51) Li, L.; Qin, X.; Mei, H.; Liu, L.; Zheng, S. Reprocessed and Shape Memory Networks Involving Poly(Hydroxyl Ether Ester) and Polydimethylsiloxane through Diels-Alder Reaction. *Eur. Polym. J.* **2021**, *160*, 110811. https://doi.org/10.1016/j.eurpolymj.2021.110811.
(52) Gou, Z.; Zuo, Y.; Feng, S. Thermally Self-Healing Silicone-Based Networks with Potential Application in Recycling Adhesives. *RSC Adv.* **2016**, *6* (77), 73140–73147. https://doi.org/10.1039/C6RA14659G.
(53) Nasresfahani, A.; Zelisko, P. M. Synthesis of a Self-Healing Siloxane-Based Elastomer Cross-Linked via a Furan-Modified Polyhedral Oligomeric Silsesquioxane: Investigation of a Thermally Reversible Silicon-Based Cross-Link. *Polym. Chem.* **2017**, *8* (19), 2942–2952. https://doi.org/10.1039/C7PY00215G.
(54) Zhao, J.; Xu, R.; Luo, G.; Wu, J.; Xia, H. A Self-Healing, Re-Moldable and Biocompatible Crosslinked Polysiloxane Elastomer. *J. Mater. Chem. B* **2016**, *4* (5), 982–989. https://doi.org/10.1039/C5TB02036K.
(55) Ishida, K.; Weibel, V.; Yoshie, N. Substituent Effect on Structure and Physical Properties of Semicrystalline Diels–Alder Network Polymers. *Polymer* **2011**, *52* (13), 2877–2882. https://doi.org/10.1016/j.polymer.2011.04.038.
(56) Hammer, L.; Van Zee, N. J.; Nicolaÿ, R. Dually Crosslinked Polymer Networks Incorporating Dynamic Covalent Bonds. *Polymers* **2021**, *13* (3), 396. https://doi.org/10.3390/polym13030396.
(57) Yu, F.; Cao, X.; Du, J.; Wang, G.; Chen, X. Multifunctional Hydrogel with Good Structure Integrity, Self-Healing, and Tissue-Adhesive Property Formed by Combining Diels–Alder Click

Reaction and Acylhydrazone Bond. *ACS Appl. Mater. Interfaces* **2015**, *7* (43), 24023–24031. https://doi.org/10.1021/acsami.5b06896.

(58) Berg, G. J.; Gong, T.; Fenoli, C. R.; Bowman, C. N. A Dual-Cure, Solid-State Photoresist Combining a Thermoreversible Diels–Alder Network and a Chain Growth Acrylate Network. *Macromolecules* **2014**, *47* (10), 3473–3482. https://doi.org/10.1021/ma500244r.

(59) Polgar, L. M.; van Duin, M.; Broekhuis, A. A.; Picchioni, F. Use of Diels–Alder Chemistry for Thermoreversible Cross-Linking of Rubbers: The Next Step toward Recycling of Rubber Products? *Macromolecules* **2015**, *48* (19), 7096–7105. https://doi.org/10.1021/acs.macromol.5b01422.

(60) Argyle, M.; Bartholomew, C. Heterogeneous Catalyst Deactivation and Regeneration: A Review. *Catalysts* **2015**, *5* (1), 145–269. https://doi.org/10.3390/catal5010145.

(61) Zhang, L.; Xu, Z.; Wei, Q.; He, S. Effect of 200keV Proton Irradiation on the Properties of Methyl Silicone Rubber. *Radiat. Phys. Chem.* **2006**, *75* (2), 350–355. https://doi.org/10.1016/j.radphyschem.2004.09.022.

(62) Cash, J. J.; Kubo, T.; Dobbins, D. J.; Sumerlin, B. S. Maximizing the Symbiosis of Static and Dynamic Bonds in Self-Healing Boronic Ester Networks. *Polym. Chem.* **2018**, *9* (15), 2011–2020. https://doi.org/10.1039/C8PY00123E.

(63) Huszank, R.; Szikra, D.; Simon, A.; Szilasi, S. Z.; Nagy, I. P. $^{4}He^{+}$ Ion Beam Irradiation Induced Modification of Poly(Dimethylsiloxane). Characterization by Infrared Spectroscopy and Ion Beam Analytical Techniques. *Langmuir* **2011**, *27* (7), 3842–3848. https://doi.org/10.1021/la200202u.